Biochemistry

Article

Cite This: *Biochemistry* 2018, 57, 5851−5863

pubs.acs.org/biochemistry

The Osmolyte TMAO Modulates Protein Folding Cooperativity by Altering Global Protein Stability

Prashant N. Jethva[†] and Jayant B. Udgaonkar*[,†,‡]

[†]National Centre for Biological Sciences, Tata Institute of Fundamental Research, Bengaluru 560065, India

[‡]Indian Institute of Science Education and Research, Pune 411008, India

Supporting Information

ABSTRACT: The folding of many globular proteins from the unfolded (U) to the native (N) state appears to be describable by a two-state N ↔ U model, which has led to the general belief that protein folding occurs in a highly cooperative manner. One reason for the widespread belief in "two-state folding" is that protein folding reactions are invariably studied by ensemble averaging probes and not by probes that can distinguish as well as quantify the multiple conformations that may be present. Consequently, how cooperativity is affected by protein stability, protein sequence, and solvent conditions is poorly understood. In this study, hydrogen exchange coupled to mass spectrometry (HX-MS) of the PI3K SH3 domain was carried out in the presence of a stabilizing osmolyte, trimethylamine *N*-oxide (TMAO). By showing that HX occurs under the EX1 regime even in the presence of 2 M TMAO, we were able to examine the temporal evolution of the populations of the different conformations present together. A strong link between protein folding cooperativity and protein stability is revealed. Increasing stability is accompanied by an increase in the ruggedness of the free energy landscape as well as diminished cooperativity; the number of amide sites simultaneously opening up their structure decreases with an increase in TMAO concentration. A comparison of the effect of TMAO to that of urea on the intrinsic dynamics of the PI3K SH3 domain indicates that TMAO counteracts the effect of urea not only on protein stability but also on protein folding cooperativity.

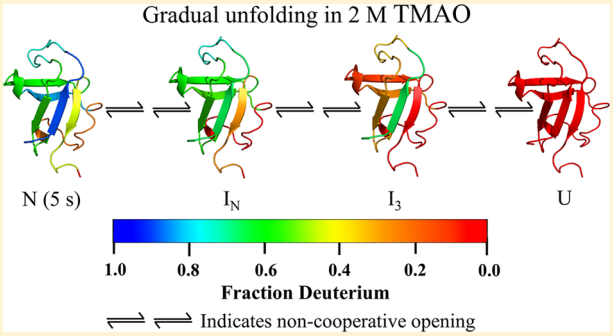

Proteins sample many partially to completely unfolded conformational states of high free energy under native conditions, according to their Boltzmann distribution.[1−6] It is still not understood whether the transition to each of the partially unfolded intermediate states is cooperative or noncooperative in nature. Moreover, the factors that determine the extent of cooperativity are not well understood.[7] It seems that a dynamic coupling between long-range (hydrophobic and electrostatic) and short-range (main chain hydrogen bonding) interactions defines the overall cooperativity (smoothness) of the folding free energy landscape. Strong coupling would lead to highly cooperative folding (two-state folding), with one large thermodynamic barrier separating the two ground (N and U) states on the folding free energy landscape. On the other hand, partial coupling would lead to reduced cooperativity (multistate folding), with more than one thermodynamic barrier separating the two ground states, while the absence of coupling would lead to an absence of cooperativity and a continuum of partially folded intermediate states, with many small thermodynamic barriers separating two ground states.[8,9] Protein stability appears to be a major factor in determining cooperativity,[10−13] and factors that affect protein stability, such as changes in solvent conditions, pressure, and temperature, are expected to modulate cooperativity.[11] A common class of cosolvents that alter protein stability are the osmolytes, but little about how osmolytes modulate the cooperative nature of the protein folding reaction is known.

Stabilizing osmolytes are small chemical molecules, including methyl amines, amino acids, and polyols, which have been selected evolutionarily to help organisms to cope with the protein denaturing effects of environmental stress.[10,14,15] Trimethylamine *N*-oxide (TMAO) belongs to the methyl amine class of osmolytes and stabilizes proteins against urea-induced denaturation under osmotic stress conditions.[14,16] How TMAO stabilizes proteins is poorly understood. Stabilization could occur because of the dominant unfavorable interaction between TMAO and the polypeptide backbone.[17−20] Alternatively, TMAO could effect a change in water structure or act through a nanocrowding mechanism.[21,22] TMAO stabilizes folding intermediates[23] and accelerates the folding of proteins.[18,24−26] Because water−water hydrogen bonding appears to become stronger than protein−water hydrogen bonding in the presence of TMAO,[19] the osmolyte is expected to modulate both the stability and dynamics of the native state and, thereby, the cooperativity of folding.[11−13,27]

Received: June 26, 2018
Revised: August 13, 2018
Published: September 10, 2018

DOI: 10.1021/acs.biochem.8b00698
Biochemistry 2018, 57, 5851−5863

Under most experimental conditions, the native (N) state or the unfolded (U) state is predominantly present, obscuring the presence of sparsely populated, high-free energy, intermediate states whose presence or absence defines the cooperativity of the folding reaction. Delineating the cooperativity of the formation of such intermediate states requires a probe that can detect these intermediates in transient coexistence with the N and/or U states. While experimental probes such as hydrogen exchange,[28,29] thiol labeling,[6,30,31] and nuclear magnetic resonance (NMR) spectroscopy[32,33] have proven to be invaluable for characterizing such transient intermediate states, it is hydrogen exchange coupled to mass spectrometry (HX-MS) that is the method of choice for providing information about the dynamics of conformational conversion between coexisting populations of different states and, hence, the cooperativity of protein folding reactions even under native conditions.[11,13,34−36]

SH3 domains are small globular proteins and are considered to be archetypal of two-state folding proteins.[37] They play important roles in signal transduction, where they provide the interaction surface for multimeric protein complexes.[38,39] The SH3 domain of the PI3 kinase was initially characterized as a cooperatively folding protein (two-state folder),[37,40] but subsequent equilibrium and kinetic folding studies showed that it (un)folds via multiple intermediate states.[41−46] Previous unfolding studies using HX-MS as a probe have shown that the unfolding of the PI3K SH3 domain is a highly heterogeneous process.[13,47] The initial structure opening events occur through a continuum of intermediate states. Only at a later stage does the remaining structure unfold in a cooperative manner. Furthermore, structural characterization of the unfolding events has shown that the cooperatively unfolding/folding core of the protein comprises β strands 1, 2, and 3 in the absence of denaturant and β strands 1, 2, 3, and 4 in the presence of 5 M urea. In this manner, the extent of folding cooperativity is greater under strongly destabilizing conditions.[13]

In the study presented here, the native state dynamics of PI3K SH3 domain was studied in the absence and presence of increasing concentrations of TMAO. In the absence of TMAO, the PI3K SH3 domain samples two partially unfolded intermediate states (I_N and I_2) noncooperatively. The cooperative opening of I_2 leads to the global unfolding of the PI3K SH3 domain. The cooperative nature of the opening of I_2 suggests that under native conditions, the unfolding of the PI3K SH3 domain is a barrier-limited transition. Upon stabilization by TMAO, the cooperativity of folding was found to decrease. Under very strongly stabilizing conditions, the PI3K SH3 domain no longer unfolds cooperatively. In 2 M TMAO, there does not appear to be any large kinetic barrier for unfolding but instead many small distributed barriers. Furthermore, an additional partially unfolded intermediate state (I_3) is sampled, suggesting that the change in thermodynamic stability also modulates the ruggedness of the free energy landscape.

MATERIALS AND METHODS

Buffers, Chemical Reagents, and Experimental Conditions. Buffers and chemical reagents, including TMAO, were of the highest purity grade and procured from Sigma-Aldrich (St. Louis, MO). Guanidine hydrochloride (GdnHCl) of the highest purity grade was procured from United States Biochemicals (USB) (Cleveland, OH). Sodium phosphate (50−100 mM) and 3-(*N*-morpholino)propanesulfonic acid (MOPS) (50 mM) were used as buffers at pH 7.2 and 6.2, respectively. The concentrations of the stock solutions of GdnHCl and TMAO[48] were determined by measuring the refractive index on an Abbe refractometer (Thermo Scientific, Waltham, MA). All the pH values mentioned were not corrected for the isotope effect. All the experiments were carried out at 25 °C.

Protein Purification. Purification of the PI3K SH3 domain was carried out as described previously.[41] The concentration of the protein was determined by measurement of the absorbance at 280 nm, using an ε_{280} of 17900 cm^{-1} M^{-1}.[49] The purity of the purified protein was checked by electrospray ionization mass spectrometry (ESI-MS) (Figure S1).

Fluorescence- and Circular Dichroism (CD)-Monitored Equilibrium Unfolding Studies. GdnHCl-induced equilibrium unfolding studies in the absence and presence of different concentrations of TMAO were carried out by monitoring the change in the intrinsic tyrosine (Tyr) fluorescence on the stopped-flow module (SFM-4, Biologic, Science Instruments, Seyssinet-Pariset, France). Tyrosine residues were excited at 268 ± 1 nm (1 cm path length), and emission was collected using a 300 ± 10 nm band-pass filter (Asahi Spectra, Torrance, CA). The protein concentration was 15−25 μM. The equilibrium unfolding curves were fitted to a two-state (N ↔ U) model (see the data analysis in the Supporting Information). Far-ultraviolet (far-UV) circular dichroism spectra were acquired using a Jasco J-815 spectropolarimeter (0.2 cm path length). The protein concentration used for far-UV CD measurements was 20−25 μM.

Deuteration of Protein. The protein was deuterated in the manner described previously.[13] In brief, the protein was dissolved in D_2O-containing buffer at pH 7.2, followed by a temperature jump to 70 °C for 10 min. The protein was then immediately placed in ice for 25 min. Finally, the deuterated protein was equilibrated at 25 °C before the start of the experiment. Protein integrity after deuteration was checked by far-UV CD spectroscopy (see Figure S2).

Hydrogen Exchange Kinetics. The hydrogen exchange (HX) reaction was initiated by diluting deuterated protein (500 μM, pH 7.2) 20-fold with protonated exchange buffer (with and without different concentrations of TMAO at pH 7.2 and 25 °C). For the back-exchange (BKEX) control, deuterated buffer at the same pH was used instead of protonated buffer. At the specified time of HX, the reaction mixture was injected into a G-25, Hi-trap (GE Healthcare, Chicago, IL) desalting column coupled to an ÄKTA basic high-performance liquid chromatograph (GE healthcare). The protein was eluted from the column using Milli-Q water acidified to pH 2.6; 50 μL of desalted and quenched protein was injected via a 50 μL loop, into the HDX module attached to a nanoAquity ultraperformance liquid chromatograph (Waters, Milford, MA), coupled with a Synapt G2 HD mass spectrometer (Waters). The protein was first collected in a C-18 reverse phase trap column at a flow rate of 75 μL/min followed by elution with a gradient from 3 to 40% acetonitrile in 2 min, at a flow rate of 40 μL/min inside the HDX module. The eluted protein was infused directly into the Synapt G2 mass spectrometer. The entire HDX module was maintained at 4−8 °C, to minimize back-exchange of deuteriums during chromatography.

DOI: 10.1021/acs.biochem.8b00698
Biochemistry 2018, 57, 5851−5863

Instrument Parameters. The capillary voltage, desolvation temperature, and source temperature of the Synapt G2 mass spectrometer were set at 3 kV, 100 °C, and 35 °C, respectively, during the acquisition of HX mass spectra. Blank runs between two HX reactions were carried out to ensure that there was no carryover from the previous run.

Data Analysis. *Intact Protein Analysis.* Twenty scans (of 1 s each) from the TIC (total ion count) chromatogram were combined to obtain the protein mass spectrum. Each mass spectrum was further analyzed with MassLynx (version 4.1, Waters) using the background subtraction, smoothing, and centroid functions. The highest-intensity charge state (+11 charge state) signal was normalized with respect to the total area under the curve using Origin (version 8, Origin Lab Corp., Northampton, MA). Unimodal and bimodal mass distributions were fitted to a single Gaussian distribution equation (eq 1) and the sum of two Gaussian (eq 2) distribution equations, respectively. Parameters (centroid mass and area under the curve) for both mass distributions were analyzed separately. The mass of the protonated protein (9276 Da) was subtracted from the observed mass of the protein at a particular time of HX to obtain the number of protected deuteriums. The number of protected deuteriums (in the high-mass distribution) as a function of time of HX was fitted to a double- or triple-exponential decay equation to obtain apparent rate constants and amplitudes of each kinetic phase of exchange. The change in the area under the low-mass distribution (fraction unfolded) as a function of time was fitted to a single-exponential equation. The peak width at 20% of the mass distribution height was obtained using HXExpress-2, an Excel-based macro program.[50,51] All the plots and fitting of data were carried out using SigmaPlot (version 12, Systat Software, San Jose, CA).

Mass distributions were fit to the following equations.

$$M_{(t)} = \frac{A_1}{\sqrt{\pi/2} \times w_1} \times e^{-2(C-C_1)^2/w_1^2} \quad (1)$$

where $M_{(t)}$ is the mass distribution at time t, A_1 is the area under the distribution, C_1 is the centroid of the mass distribution at time t, w_1 is the full width at half-maximum of the Gaussian distribution, and C is the linearly variable m/z axis.

$$M_{(t)} = \left[\frac{A_1}{\sqrt{\pi/2} \times w_1} \times e^{-2(C-C_1)^2/w_1^2}\right] + \left[\frac{A_2}{\sqrt{\pi/2} \times w_2} \times e^{-2(C-C_2)^2/w_2^2}\right] \quad (2)$$

where $M_{(t)}$ is the mass distribution at time t, A_i, C_i, and w_i are the area under the distribution, the centroid, and the peak width at half-maximum for each Gaussian distribution i, respectively, and C is the linearly variable m/z axis.

Peptide Analysis. For peptide analysis, the protein was digested by being passed through an immobilized pepsin column (Applied Biosystems, Foster City, CA) kept inside the HDX module. The protein was passed through the pepsin column at a flow rate of 50 μL/min for 4 min with Milli-Q water containing 0.05% formic acid. Protein fragments thus generated were initially trapped inside a C-18 reverse phase trap column, followed by separation using a C-18 reverse phase analytical column (gradient from 10 to 40% acetonitrile containing 0.1% formic acid) over 10 min. The MS/tandem MS^E method was used to obtain the MS/MS spectra of different protein fragments. The ProteinLynx Global Server (PLGS, version 2.4, from Waters) was used to identify each peptide and its retention time from the MS/MS mass spectrum.

To determine the centroid mass, as well as the width at 20% of the peak height of the isotopic mass distribution, intensity values for the isotopic mass distributions were exported to HX-Express2. The isotopic mass distributions were fitted to a single binomial function. The fractional deuterium content in each sequence segment was calculated according to eq 3.

$$\text{fraction D} = \frac{m_{(t)} - m_{(5\%\,\text{D})}}{m_{(100\%\,\text{D})} - m_{(5\%\,\text{D})}} \quad (3)$$

where $m_{(t)}$ is the observed centroid mass at time t of HX. The centroid mass of each peptide in the BKEX control sample was considered as the 100% deuterated control, and the centroid mass of each peptide at 180 d (days) of exchange was considered as the 5% deuterated control. The plot of the fraction of deuterium retained as a function of time was fitted to a single-, double-, or triple-exponential decay equation to determine the apparent rate constants and amplitudes of the HX reaction.

RESULTS

TMAO Stabilizes the PI3K SH3 Domain. The PI3K SH3 domain has seven Tyr residues dispersed throughout the protein sequence. Tyr fluorescence is quenched by the single tryptophan (Trp) residue in the folded state of the protein due to fluorescence resonance energy transfer (FRET). Hence, the Tyr fluorescence spectrum is a good tool for monitoring the tertiary structure of the protein. Figure 1 shows Tyr fluorescence-monitored GdnHCl-induced equilibrium unfolding curves in the presence of increasing concentrations of TMAO. Each equilibrium unfolding curve fit well to a two-state (N ↔ U) model. The parameters obtained from the fits, the free energy of unfolding (ΔG_{NU}) and the midpoint of the transition (C_m), increased linearly with an increase in the

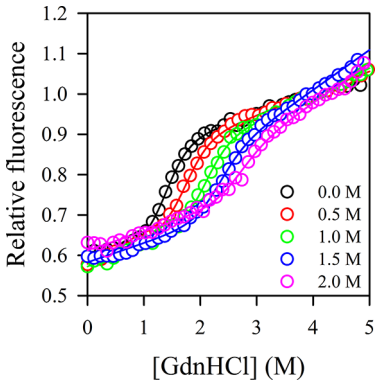

Figure 1. Equilibrium unfolding studies of the PI3K SH3 domain in the absence and presence of different concentrations of TMAO at pH 7.2 and 25 °C. Shown are tyrosine fluorescence-monitored, GdnHCl-induced equilibrium unfolding curves in the presence of increasing concentrations of TMAO. These were normalized by the fluorescence signal at 4 M GdnHCl. The solid lines represent fits to a two-state model for unfolding (see Figure S3 for the parameters obtained from the fits).

DOI: 10.1021/acs.biochem.8b00698
Biochemistry 2018, 57, 5851−5863

concentration of TMAO (Figure S3). The value of m_{eq}, which is a measure of the change in the solvent accessible surface area upon unfolding, was found to decrease in the presence of TMAO. This suggested that the U state becomes compact upon addition of TMAO.

It should be noted that upon addition of TMAO, the fluorescence emission spectra of the native (N) and unfolded (U) proteins showed no change in their emission maxima (Figure S4). However, a gradual decrease in the Tyr fluorescence intensity and a concomitant increase in the Trp fluorescence intensity were observed for the U state in the presence of increasing concentrations of TMAO. This increase in the level of fluorescence resonance energy transfer from Tyr to Trp suggests that the U state becomes more compact in the presence of TMAO. Tyr fluorescence also decreased for the native protein in the presence of TMAO; however, a concomitant increase in Trp fluorescence was not observed. Figure S4 also shows that the secondary structure of the native and unfolded proteins remained unperturbed upon addition of TMAO. It is also seen that the protein remains fully soluble, in its native and unfolded states, even in 2 M TMAO (Figure S4B,D).

Effect of TMAO-Induced Stabilization on Mass Distributions. The HX reaction in the absence and presence of TMAO was carried out by diluting the deuterated protein into the protonated exchange buffer at the same pH. At a specific time of HX, the reaction was quenched by desalting followed by the acquisition of the mass spectrum. Figure 2 and Figure S5 show the mass distributions [+11 charge state, the most intense charge state (Figure S1)] at different times of HX in the absence and presence of different concentrations of TMAO. The unimodal mass distributions at the earliest time point of HX (5 s) indicated the presence of only one population of the native protein in the absence and presence of TMAO. As was shown previously,[13] in the absence of TMAO, the mass distribution remained unimodal during the initial 300 s of HX and shifted gradually to a lower mass (Figure 2, 0 M TMAO). After 300 s, the mass distribution became bimodal with the appearance of a lower mass distribution corresponding to the completely exchanged out protein (unfolded state). The observation of the bimodal mass distribution suggested that the protein undergoes cooperative structural opening in the absence of TMAO. To further validate the observations described above, the charge state distributions at all time points of HX in the absence of TMAO were deconvoluted and analyzed. Figure S6 shows that the deconvoluted mass distributions also behaved in a manner similar to that of the mass distributions of the +11 charge state.

The presence of TMAO resulted in a significant change in the observed mass distributions (Figure 2). As in the absence of TMAO, the mass distribution was observed to shift gradually up to 300 s of HX, and at later time points, the mass distribution became bimodal. Bimodality in the mass distributions was observed at TMAO concentrations of ≤1.5 M, suggesting that unfolding occurs in a barrier-limited cooperative manner. However, in the presence of 2 M TMAO, the mass distribution remained unimodal at all times of HX, suggesting that under the most stabilizing solvent conditions, the protein exchanged out all its protected deuteriums by noncooperative openings only.

Figure 2 shows that the two components of the bimodal mass distribution were very well separated on the m/z scale in the absence of TMAO but that in the presence of increasing

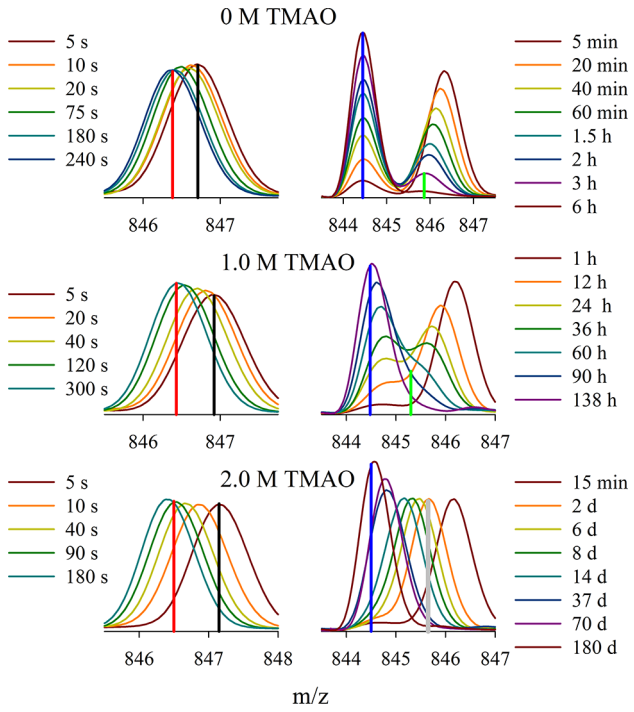

Figure 2. Kinetics of HX into the intact PI3K SH3 domain in the absence and presence of different concentrations of TMAO at pH 7.2 and 25 °C. Representative mass distributions corresponding to the +11 charge state are shown for early and later time points of HX, for each experimental condition. The black, red, green, and blue solid vertical lines represent the centroid m/z values for the N state (5 s), for partially unfolded intermediate states populated at the end of the fast (I_N) and slow (I_2) noncooperative phases of HX, and for the globally unfolded state U, respectively. The gray solid vertical line for mass distributions in the presence of 2.0 M TMAO represents the centroid m/z for the partially unfolded state (I_3) populated at the end of the additional noncooperative phase of HX.

concentrations of TMAO, the two components begin to merge with each other. To quantify this behavior, the change in the peak width of the bimodal mass distribution was analyzed. An analysis of the kinetics of this change can provide valuable information about the cooperative nature of a protein folding reaction.[52] It is seen from the kinetics (Figure S7) that at the initial time points of HX, the peak width was constant but increased at later time points due to the appearance of the low mass distribution. The magnitude of the increase in the peak width gave the number of cooperatively opening residues. This difference was 15 ± 1, 13 ± 1, 8 ± 1, and 6 ± 1 Da for 0, 0.5, 1.0, and 1.5 M TMAO, respectively, suggesting that the cooperativity of folding decreased in a TMAO concentration-dependent manner. The absence of a peak width maximum for HX in the presence of 2 M TMAO indicated a complete loss of protein folding cooperativity. It should be noted that the protein remained soluble and stable during prolonged incubation in the presence of 2 M TMAO (Figure S8)

Effect of TMAO-Induced Stabilization on the Kinetics of Hydrogen Exchange. Figure 3 shows that in the absence of TMAO, the high mass distributions shifted gradually to low mass in two kinetic phases, the fast and slow phases of noncooperative HX. At later time points, HX appeared to occur cooperatively. The area under the low mass distribution increased in an exponential manner (Figure 3A,F). The fast and slow phases of noncooperative HX into the species giving

DOI: 10.1021/acs.biochem.8b00698
Biochemistry 2018, 57, 5851−5863

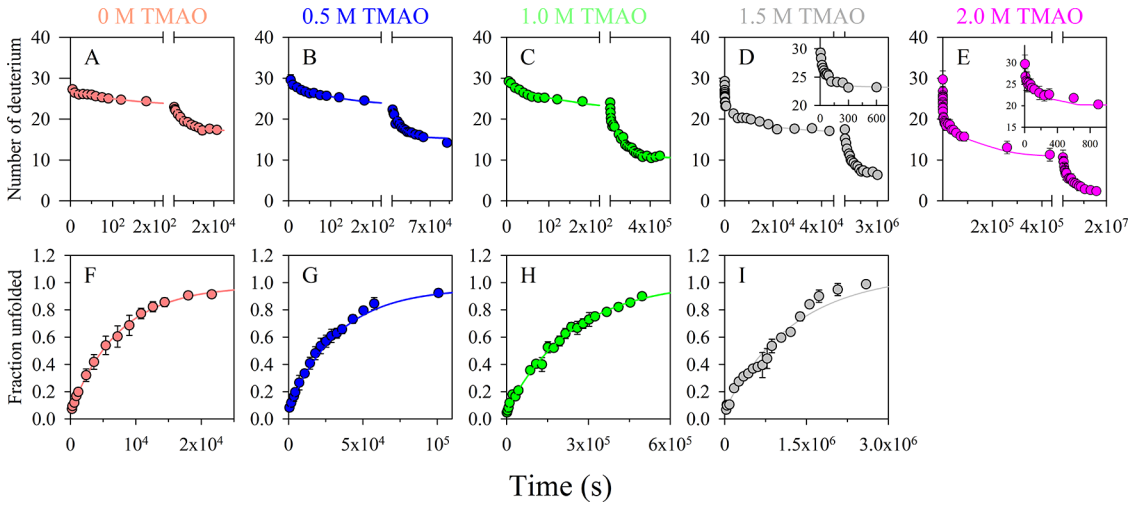

Figure 3. Kinetics of HX into the PI3K SH3 domain in the absence and presence of different concentrations of TMAO at pH 7.2 and 25 °C. The solid lines in panels A−C are fits to a double-exponential equation and in panels D and E are fits to a triple-exponential equation. The insets in panels D and E show early time points of HX. The solid lines through the fraction unfolded data in panels F−I are fits to a single-exponential equation. The apparent rate constants and amplitudes of each kinetic phase of the HX reaction are listed in Table S1. The fraction unfolded (and, thereby, the global unfolding rate) could not be obtained from HX measurements in the presence of 2 M TMAO because the mass distributions were unimodal at all times of HX. At the end of HX reactions, the protein was found to retain 2 ± 1 deuteriums at pH 7.2 and 25 °C. This was expected because the HX reactions were carried out in a buffer containing 5% D_2O and 95% H_2O. The error bars represent the spread in the data from two separate experiments.

rise to the high mass distribution indicated that the N state transiently sampled partially unfolded intermediate states I_N (fast phase) and I_2 (slow phase), as had been shown previously.[13] The slow phase of cooperative HX suggested that global opening of I_2 led to the sampling of the U state. It was seen that the apparent rate constants for the slow noncooperative formation of I_2 and cooperative formation of U were similar (Table S1). Eighteen ± 1 deuteriums were found to exchange cooperatively in the absence of TMAO, as also seen previously.[13] Many SH3 domains are known to undergo partial cooperative unfolding.[53] The half-life (apparent rate) of global unfolding of the PI3K SH3 domain is in good agreement with the previously reported half-lives of other SH3 domains.[54]

In the presence of 0.5 (Figure 3B,G) and 1.0 M TMAO (Figure 3C,H) also, the high mass distribution shifted into two kinetic phases and the cooperative opening of I_2 led to global unfolding. When HX was carried out in the presence of TMAO, the kinetic phases corresponding to the formation of I_2 and U were slower than in the absence of TMAO. The important difference between HX in the absence and HX in the presence of TMAO was the decrease in the number of cooperatively opening residues, which was 15 ± 1 and 11 ± 1 in 0.5 and 1 M TMAO, respectively, in good agreement with the numbers obtained from the peak width analysis (Figure S7)

In 1.5 M TMAO also, bimodal mass distributions were observed at later times of HX. Unlike the case of HX at lower TMAO concentrations, however, the gradual shift in the high mass distribution was found to occur in three kinetic phases (Figure 3D,I). This result suggested that apart from sampling I_N and I_2, the protein populated an additional partially unfolded intermediate state (I_3) in 1.5 M TMAO. The number of residues opening cooperatively was reduced even further to 7 ± 1 in the presence of 1.5 M TMAO.

When HX was carried out in the presence of 2 M TMAO, the mass distribution was found to remain unimodal throughout the exchange process. The kinetics of the change in the number of protected deuterium fit to a triple-exponential decay equation (Figure 3E). Thus, the protein lost all its protected deuteriums in a noncooperative (diffusive) manner and sampled even the U state by noncooperative diffusive opening of the polypeptide backbone. The apparent rate constants for the formation of I_2 and U were very similar. The triple-exponential decay suggested that in the presence of 2 M TMAO, the protein exchanges during the noncooperative formation of I_N, I_3, and U.

Mechanism of HX in the Presence of TMAO. To determine whether structural openings are noncooperative or cooperative, it is necessary to know whether HX in a particular solvent condition occurs in the EX1 or EX2 regime (see the Supporting Information). When HX occurs in the EX1 regime, it becomes possible to distinguish cooperative from noncooperative structural unfolding.[11,36,55,56] The most definitive way to identify the HX regime is to measure the pH dependence of the observed apparent rate constant of HX (see the text of the Supporting Information). In the case of TMAO concentrations of ≤1.5 M, the mass distribution showed bimodality at later time points of HX. This suggested that for these lower TMAO concentrations, HX occurs in the EX1 regime. To determine which HX regime was operative in the presence of 2 M TMAO, where only unimodal mass distributions were observed, HX in the presence of 2 M TMAO was also carried out at pH 6.2 and 25 °C. In the EX2 regime, the observed apparent rate constant of HX is expected to decrease 10-fold with a decrease in the pH of the HX reaction by 1 unit, while in the EX1 regime, it is expected to remain constant.[57] Figure 4 and Table S1 show that the apparent rate constants and the numbers of deuteriums exchanged during all three kinetic phases of HX in the presence of 2 M TMAO were similar at pH 6.2 and 7.2, suggesting that HX occurs in the EX1 regime in the presence of 2 M TMAO. It should be noted that the protein stability is

DOI: 10.1021/acs.biochem.8b00698
Biochemistry 2018, 57, 5851−5863

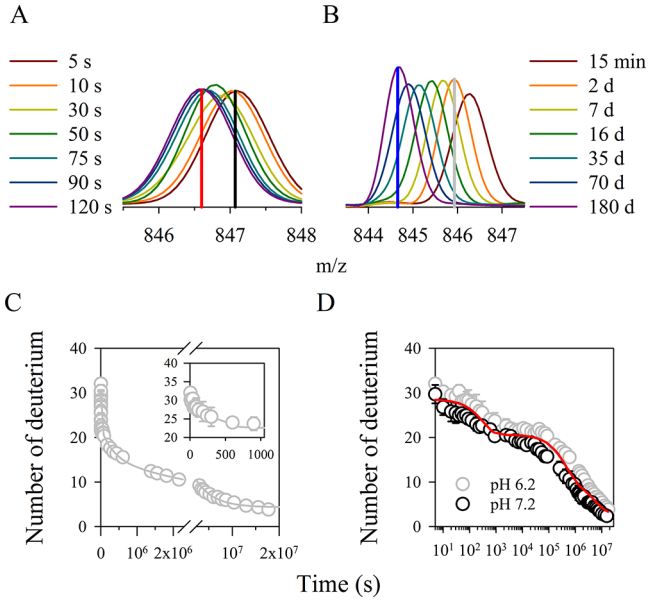

Figure 4. HX into the PI3K SH3 domain in the presence of 2 M TMAO at pH 6.2 and 25 °C. Representative mass distributions (+11 charge state) are shown in panels A (early time points of HX) and B (later time points of HX). The black, red, gray, and blue vertical solid lines indicate the centroid m/z of N (5 s) and partially unfolded states populated at the end of the fast noncooperative phase (I_N), at the end of the additional noncooperative phase (I_3), and in the U state, respectively. Panel C shows the change in number of deuteriums with time of HX. More deuteriums were retained by the native state at pH 6.2 than at pH 7.2. The gray solid line is a fit of to the data to a three-exponential equation. The inset shows the early time pointes of HX. See Table S1 for the apparent rate constants and amplitudes of the HX reaction. Panel D compares the changes in the numbers of deuteriums with time of HX at pH 7.2 (black circles) and pH 6.2 (gray circles), plotted vs time of HX. The red solid line is a global fit of the data at both pH values to a three-exponential equation (for more details, see Table S1). At the end of the HX reactions, the protein was found to retain 2 ± 1 deuteriums at pH 6.2 and 25 °C. This was expected because the HX reactions were carried out in a buffer containing 5% D_2O and 95% H_2O. The error bars represent the spread in the data from two separate experiments.

very similar at both pH 6.2 and 7.2 at 25 °C in the presence of 2 M TMAO (Figure S9).

However, a mere comparison of the apparent rate constants of HX at two different pH values for only the intact protein may not provide a correct picture of the HX regime. Therefore, the pH dependencies of the apparent rate constants of HX into different sequence segments of the protein were determined. To study the kinetics of HX into different sequence segments in the presence of 2 M TMAO, pepsin proteolysis of the protein was carried out at pH 2.6 after the HX reaction was quenched. Figure S10 shows the different sequence segments, which were separated by reverse phase chromatography (RP-LC) followed by identification through mass spectrometry (MS). To obtain quantitative information from isotopic mass distributions arising from the different sequence segments, each isotopic mass distribution was fitted to a single binomial equation to obtain the width and centroid. From the centroid mass, the fraction of deuterium retained, averaged over all the amide sites within the sequence segment, was obtained (see Materials and Methods).

Figures S11 and S12 show that as in the case of the whole intact protein, all the sequence segments showed a gradual shift in unimodal mass distributions (noncooperative opening) at all time points of HX at pH 7.2 and 6.2. The kinetics of the change in the fraction of deuterium retained were identical at pH 7.2 and 6.2 for most of the sequence segments, and hence, global fits of the HX data were carried out, except for sequence segment 71−81 (β strand 5) (Figure S13). The apparent rate constants obtained from the global fits were very similar to the apparent rate constants obtained at pH 7.2 (Figure 5 and Table S2). Hence, as in the case of HX into the whole intact protein, HX into individual sequence segments was also independent of pH. HX into sequence segment 71−81 could be described by a two-exponential equation, and the apparent rate constants of the fast and slow phases of noncooperative HX at pH 6.2 were more than 10- and 3-fold slower, respectively, than the apparent rate constant at pH 7.2. This suggested that for this sequence segment only, HX occurred in the EX2 regime during the fast phase and in the EXX regime during the slow phase of noncooperative HX. Furthermore, to identify any subtle changes in the mass distributions due to the change in pH during HX, the kinetics of the change in peak width during HX into different sequence segments were determined. Figure S14 shows that all the sequence segments showed very similar peak widths at both pH values at all times

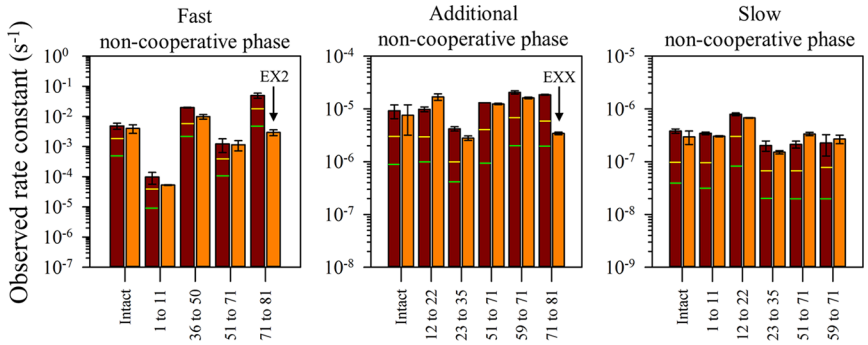

Figure 5. Comparative analysis of kinetics of HX into the PI3K SH3 domain in the presence of 2 M TMAO at pH 7.2 and 6.2 at 25 °C. The apparent rate constants of each kinetic phase of HX at pH 7.2 (dark brown bars, Figure 7) were compared to the apparent rate constants obtained from the global fit of pH 7.2 and 6.2 HX kinetics (light brown bars) in the presence of 2 M TMAO (Figure S13 and Table S2). For sequence segments 36−50 and 71−81, the data at pH 7.2 and 6.2 were fitted separately to obtain the apparent rate constants and amplitudes. The yellow and green horizontal lines on the dark brown bars correspond to rate constants that are 3- and 10-fold slower, respectively, than the observed rate constant at pH 7.2. The error bars represent the spread in the data from two separate experiments.

DOI: 10.1021/acs.biochem.8b00698
Biochemistry 2018, 57, 5851−5863

of exchange. These observations suggested that in the presence of 2 M TMAO, HX did indeed occur in the EX1 regime.

TMAO Dependence of Opening/Unfolding Rate Constants. The dependence of the kinetics of HX on TMAO concentration is a measure of the amount of TMAO-disfavored surface area in each partially unfolded intermediate state. The U state, which exposes a large amount of polypeptide backbone surface area, would be destabilized greatly by the unfavorable interaction of TMAO with the polypeptide backbone. Likewise, any intermediate state that exposes a large polypeptide backbone surface area would form with an apparent rate constant that would be greatly affected by TMAO concentration. Figure 6A shows that the logarithm

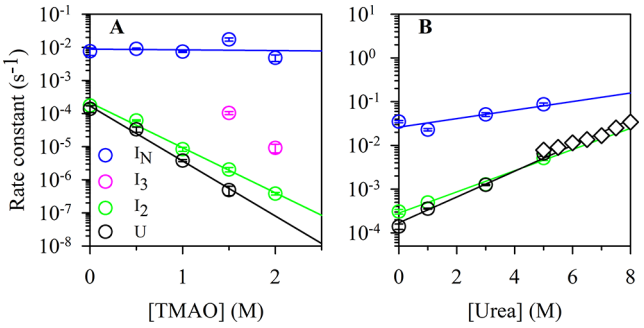

Figure 6. Dependence on TMAO and urea concentration of the apparent rate constants of the different kinetic phases of HX into the PI3K SH3 domain at pH 7.2 and 25 °C. Blue, pink, green, and black circles represent the apparent rate constants of formation of partially unfolded intermediate states I_N, I_3, and I_2 and globally unfolded state U, respectively. Black diamonds in panel B represent Tyr fluorescence-monitored apparent global unfolding rate constants in the presence of urea. The apparent rate constants of formation of I_N, I_2, and I_3 were determined from the shift in the centroid of the high mass distribution with time of HX. The apparent rate constants of global unfolding were obtained by monitoring the change in the population of completely unfolded protein with time of HX. The solid lines are linear fits to the dependence of the logarithm of the apparent rate constants on (A) TMAO and (B) urea concentration. The slopes of the dependence of the logarithm of the apparent rate constants of formation of I_N, I_2, and U on TMAO and urea concentration are −0.02, −1.36, and 1.66 M^{-1} and 0.09, 0.25, and 0.29 M^{-1}, respectively. The error bars represent the spread in the data from two separate experiments. Panel B reprinted with permission from ref 13. Copyright 2017 American Chemical Society.

of the apparent rate constant for the formation of I_N has a weak dependence on TMAO concentration. This weak dependence suggested that similar to the case of urea (Figure 6B), TMAO did not affect the TS state for the formation of I_N; hence, the apparent rate constant remained unaffected by the presence of TMAO. As previously observed for urea (Figure 6B), the logarithms of the apparent rate constants for the formation of I_2 and U were also found to have strong and similar dependencies on TMAO concentration. However, contrary to the observation made in the case of urea, where the apparent rate constants for the formation of I_2 and U became very similar at high urea concentrations, the apparent rate constants for the formation of I_2 were found to be slightly faster than those for the formation of U, at higher concentrations of TMAO (Figure 6). The dependence of the apparent rate constant of formation of I_3 on TMAO concentration could not be measured because there were insufficient data points. The observation that the global unfolding rate constant decreases with an increase in TMAO concentration suggests that the TS for global unfolding is destabilized in the presence of TMAO. While this result is consistent with TMAO interacting unfavorably with the polypeptide backbone, it is possible that TMAO also acts via other mechanisms.[21,22]

Structural Characterization of Partially Unfolded States in the Presence of 2 M TMAO. To understand how the intrinsic dynamics of different regions of the PI3K SH3 domain were modulated by the presence of 2 M TMAO, pepsin proteolysis of the protein was carried out as mentioned above. Figure S11 shows the isotopic mass distributions of different sequence segments at different times of HX in the presence of 2 M TMAO at pH 7.2 and 25 °C. The isotopic mass distributions corresponding to all the sequence segments showed the gradual shift along the m/z axis and fit well to a single binomial distribution at all time points of HX.[51] The most striking differences between HX in the absence and presence of 2 M TMAO were observed for sequence segments 1−11 (β strand 1), 23−35 (β strand 2), and 51−71 (β strands 3 and 4). All three sequence segments were known to exchange cooperatively in the absence of TMAO,[13] but they exchanged noncooperatively in the presence of 2 M TMAO. To characterize how protected deuteriums exchanged out in each sequence segment, the kinetics of the change in the fraction of deuterium retained were fit to a single-, double-, or triple-exponential decay equation. Table S2 shows the apparent rate constants and amplitudes of HX for each sequence segment.

Figure 7 shows the kinetics of HX into each sequence segment. Sequence segment 36−50 (nSrc loop) exchanged its protected deuteriums within 200 s of HX in a single-exponential phase. Sequence segments 1−11 (β strand 1), 12−22 (RT loop), 23−35 (β strand 2), 59−71 (β strand 4), and 71−81 (β strand 5) exchanged protected deuteriums in two exponential phases. The observation of two apparent rate constants of exchange for sequence segment 1−11 (β strand 1) suggests that it takes part in the formation of I_N as well as the gradual noncooperative formation of the U state. The apparent rate constants of HX into sequence segments 12−22, 23−35, and 59−71 indicate that they exchanged during the formation of I_3 and the noncooperative formation of U. The apparent rate constants for sequence segment 71−81 suggest that it exchanged during the formation of I_N and I_3 only. Sequence segment 51−71 (a β hairpin comprises β strands 3 and 4) exchanged protected deuteriums in three exponential phases (Figure 7). This suggests that it exchanged during the noncooperative formation of I_N, I_3, and U. Figure 8 maps the HX kinetics and the fraction of deuterium protected in each partially unfolded intermediate state onto the structure of the N state.

DISCUSSION

It has been suggested recently[11] that the cooperativity of unfolding can be modulated by modulating the thermodynamic stability of a protein. Under destabilizing solvent conditions, in which either GdnHCl or urea is present, it was seen that the cooperativity of unfolding of monellin[11] and of the PI3K SH3 domain[13] increased. Under stabilizing solvent conditions, cooperativity is expected to decrease. In the study presented here, it is shown that TMAO, an osmolyte known to counteract the destabilizing effect of urea, reduces the cooperativity of the unfolding of the PI3K SH3 domain.

DOI: 10.1021/acs.biochem.8b00698
Biochemistry 2018, 57, 5851−5863

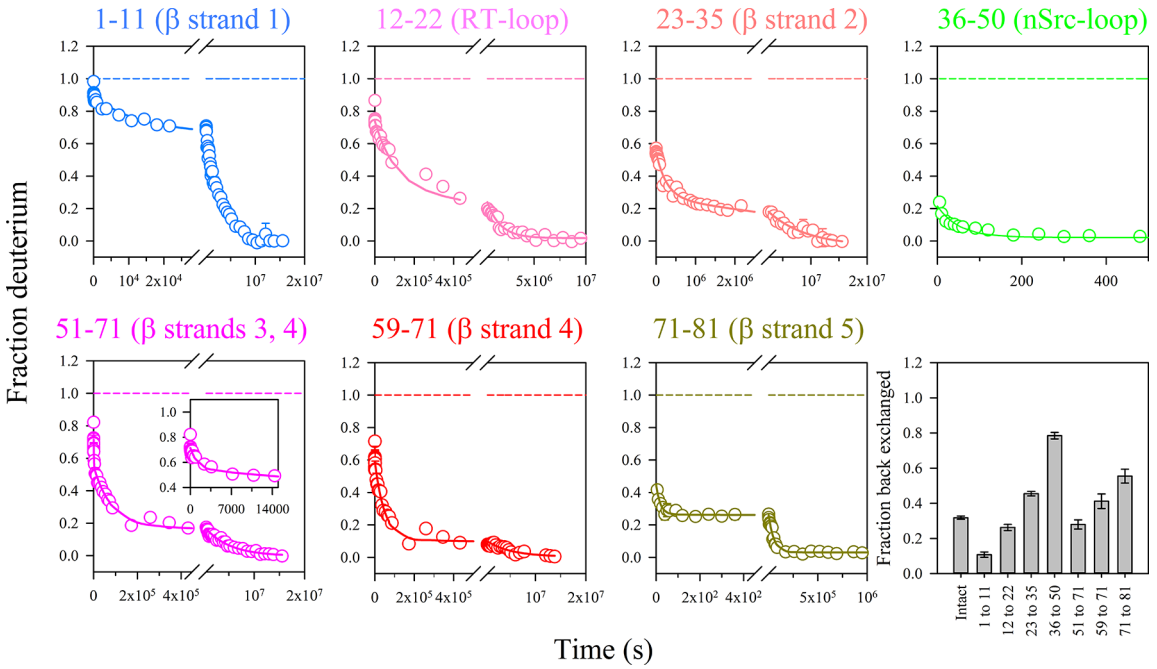

Figure 7. Kinetics of HX into different sequence segments of the PI3K SH3 domain in the presence of 2 M TMAO at pH 7.2 and 25 °C. Dashed lines are the fractions of deuterium retained (1.0) in each sequence segment in the BKEX control sample. The solid lines are fits to single-exponential (sequence segment 36−50), double-exponential (sequence segments 1−11, 12−22, 23−35, 59−71, and 71−81), and triple-exponential (sequence segment 51−71) equations. The inset for sequence segment 51−71 shows early times of HX. The bar graph shows the fraction of deuterium back-exchanged in the first 5 s of HX. The apparent rate constants and amplitudes obtained from the fits are listed in Table S2. The error bars represent the spread in the data from two separate experiments.

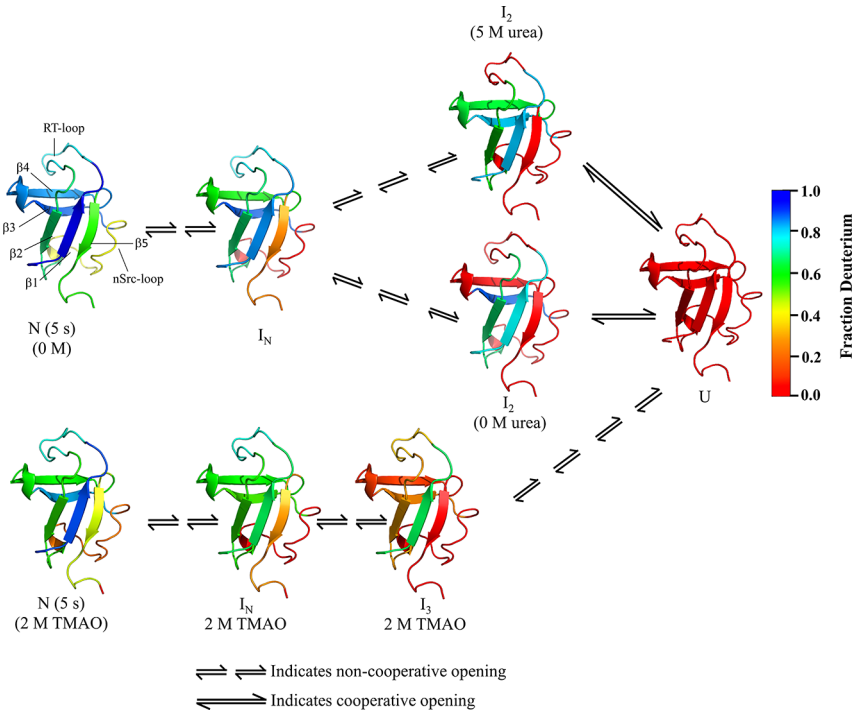

Figure 8. Comparative analysis of the structures of different partially unfolded intermediate states in the absence (0 M) of any cosolvent, under a strongly destabilizing condition (5 M urea) and under a strongly stabilizing condition (2 M TMAO) at pH 7.2 and 25 °C. The lengths of the equilibrium arrow for cooperative opening indicate the size of the cooperative unit.

Furthermore, it is also shown that upon stabilization, the energy landscape becomes more rugged.

Multiple Structural Openings of the PI3K SH3 Domain in the Absence of TMAO. As reported previously,[13] and as demonstrated in this study (Figure 4), HX occurs in the EX1 regime in the absence of TMAO. Hence, the gradual shift in the high mass distribution can be attributed to noncooperative structural openings of the N state

DOI: 10.1021/acs.biochem.8b00698
Biochemistry 2018, 57, 5851−5863

(Figure 2 and Figure S5). Such gradual, noncooperative opening of the structure could be due to the independent loss of structure at each amide residue, one at a time. The opening and closing events at the individual amide sites could be either parallel or sequential to each other. The apparent rate constant of HX obtained from the gradual shift in mass distribution would be the mean apparent rate constant of HX for all the residues that are exchanging during that particular exponential phase.

As shown previously,[13] the shift in the high mass distribution, which occurs in two kinetic phases, arises from the transient sampling of two partially unfolded high-free energy intermediates (I_N and I_2) by the N state (Figure 3). Because the apparent rate constants for the two phases are very different from each other, the transition states (TSs) preceding the formation of I_N and I_2 must be structurally very different. I_N forms the fastest, suggesting that it is nativelike it forms on the native side of the major rate-limiting barrier of unfolding. It appears that weakly protected residues near the surface of the protein exchange during the formation of I_N and that more buried residues exchange out during the formation of I_2. Once important tertiary interactions are broken, global unfolding of protein occurs, and solvent molecules penetrate the protein core and exchange fully buried amide sites. Such native state breathing openings/motions are believed to be important for protein function.[5,58−60] The apparent rate constant of formation of I_2 is very similar to the apparent rate constant of cooperative formation of U, suggesting that I_2 and U both form after the rate-limiting barrier of unfolding.[13] HX can distinguish cooperative and noncooperative opening on the same side of the rate-limiting unfolding barrier.

It should be noted that global unfolding of the PI3K SH3 domain occurs at a rate constant that is similar to that seen for other SH3 domains.[54] Other SH3 domains also fold and unfold via partially unfolded forms.[53] Transient folding intermediates populated during protein folding are considered to be important for guiding the polypeptide chain to its native state.[61,62] Furthermore, cooperative (un)folding is believed to reduce the conformational search time and to keep the polypeptide chain away from sampling the aggregation prone conformations.[63,64]

Modulating Protein Folding Cooperativity by Altering Thermodynamic Stability. It has been observed that modulation of the thermodynamic stability of the N or U state results in the modulation of the cooperativity of protein unfolding and/or folding.[11] This was shown by carrying out native state HX in the EX1 regime, in the case of both monellin[11] and the PI3K SH3 domain.[13] Unfortunately, most proteins do not undergo native state HX in the EX1 regime under physiological-like conditions. Nevertheless, earlier HX-NMR studies had indicated that the cooperativity of unfolding is coupled to denaturant concentration (unfolded state stabilization).[28] Under strongly native conditions, many residues were observed to have unique dependencies on denaturant concentration, and at higher denaturant concentrations, many HX isotherms converged. It should be mentioned that although HX-NMR provides residue specific information, it cannot provide population level information. Hence, it cannot directly delineate noncooperative structural openings from a cooperative structural opening.[34]

To understand how thermodynamic stability modulates the conformational space sampled by the PI3K SH3 domain, the stability of the protein was increased by the addition of TMAO (Figure 1), and the native state dynamics was studied by HX at increasing TMAO concentrations. It is seen that up to the increase in stability provided by the addition of 1.5 M TMAO, the mass distribution behaved qualitatively as it does in the absence of TMAO (Figure 2 and Figure S5): the protein appears to sample the same conformational space as it does in the absence of TMAO. Quantitative analysis (Figure 3 and Table S1) shows, however, that at 1.5 M TMAO the high mass distribution shifts in three kinetic phases. This suggests that apart from I_N and I_2 the protein samples an additional partially unfolded intermediate state I_3. A sampling of an additional intermediate state indicates an increase in the ruggedness of the energy landscape of the protein upon stabilization. Furthermore, the observation that the total number of noncooperatively exchanging deuteriums increases at the expense of the number of cooperatively exchanging deuteriums indicates that local unfolding dominates over global unfolding in the presence of increasing TMAO concentrations (Table S1). Upon further stabilization by the addition of 2 M TMAO, there appears to be a complete loss of cooperativity, as indicated by the observation that only unimodal mass distributions were observed at all time points of HX (Figure 2). Hence, it appears that TMAO-induced thermodynamic stabilization decreases the cooperativity of unfolding and converts an inherently cooperative unfolding transition into a completely noncooperative transition. Like TMAO, other osmolytes such as sarcosine are also expected to stabilize the PI3K SH3 domain, in a manner similar to how they stabilize other proteins.[23] Other osmolytes may also allow the visualization of previously unseen intermediates such as I_3, but this remains to be demonstrated. It is also possible that TMAO and other osmolytes may alter the structure of conformations populated on a folding pathway, as has been shown for barstar,[23] but not in the case of the Fyn SH3 domain.[65]

Previously, it had been shown that protein folding cooperativity increases upon addition of chemical denaturants.[11,13] It appears that TMAO counteracts not only the effect of a chemical denaturant such as urea[13] on stability but also the effect of urea on cooperativity.

Structure of Partially Unfolded Intermediate States under Stabilizing Conditions. It has been shown that the nSrc loop and RT loop behave as a single noncooperatively opening unit and that both exchange during the formation of I_N and I_2 in the absence of any TMAO.[13] The nSrc loop still exchanges out in a single kinetic phase (during the formation of I_N) in the presence of 2 M TMAO, too, while the RT loop exchanges out in two kinetic phases (during the formation of I_3 and U) (Figure 7). This suggests that the RT loop has at least two groups of amide sites whose protection factors differ in the presence of 2 M TMAO but not in its absence. The RT loop has a partial β sheet character: a few of its residues are involved in intraloop hydrogen bonding.[66] It is possible that these hydrogen-bonded amide sites exchange slowly under strongly stabilizing solvent conditions and do so only during the formation of U. Amide sites that have less protection because they are not hydrogen-bonded appear to exchange out during the formation of I_3. Both loop regions are known to be very dynamic in solution[66] and to expose a large surface area of the polypeptide backbone to solvent. It appears that compaction of both loops by TMAO[18,25] slows the dynamics. Non-hydrogen-bonded amide sites might be very dynamic in the absence of

DOI: 10.1021/acs.biochem.8b00698
Biochemistry 2018, 57, 5851−5863

TMAO, and hence, the RT loop exchanged out in a single kinetic phase.[13]

Sequence segments 1−11 (β strand 1), 23−35 (β strand 2), and 51−71 (β strands 3 and 4) unfold cooperatively in the absence of TMAO,[13] but they show only gradual non-cooperative openings in the presence of 2 M TMAO (Figure S11). Previously, sequence segment 1−11 was found to exchange in three kinetic phases, and the apparent rate constants of formation of I_2 and U were similar in the absence of TMAO. Thus, one fewer kinetic phase is seen for β strand 1 (Figure 7 and Table S2). β strand 2 was found to exchange out cooperatively in the absence of any TMAO. However, in the presence of 2 M TMAO, it exchanges not only non-cooperatively but also in two kinetic phases leading to the formation of I_3 and U. This is likely because β strand 2 is hydrogen bonded with β strands 1 and 3. TMAO differentially affects the intrinsic dynamics of β strands 1 and 3. β strand 1 behaves approximately the same in the absence and presence of TMAO, while the dynamics of β strand 3 is greatly affected by the presence of TMAO (see below). This asymmetric stabilization around β strand 2 appears to lead to the partitioning of amide sites within β strand 2, which then exchange out with rate constants that differ by up to an order of magnitude. In the presence of 2 M TMAO, β strand 3 exchanges out during all the three kinetic phases of HX, leading to the formation of I_N, I_3, and U, while β stand 1 exchanges out only during the formation of I_N and U. Hence, amide sites in β stand 2 that exchange out during the formation of I_3 must be coupled structurally to β strand 3, and amide sites that exchange out during the formation of U could be coupled structurally to both β stands 1 and 3.

The observation that sequence segment 51−71 exchanges out in three kinetic phases suggests that β strands 3 and 4 (β hairpin) take part in the noncooperative formation of all three states, I_N, I_3, and U. Sequence segment 59−71 (β strand 4), which is a smaller (second half) segment of sequence segment of 51−71, exchanges out in two kinetic phases, whose apparent rate constants suggest that it exchanges out during the formation of I_3 and U. This directly suggests that sequence segment 51−58 (β stand 3) of sequence segment 51−71 must exchange out during the formation of I_N. Furthermore, subtraction of the amplitude of HX for sequence segment 59−71 (β strand 4) from the amplitude of HX for sequence segment 51−71 (β strands 3 and 4) indicates that sequence segment 51−58 (β strand 3) exchanges out in all three kinetic phases, too (Table S2). This is in sharp contrast to the cooperative exchange of sequence segment 51−58 in the absence of TMAO. This change in the nature of the exchange of sequence segment 51−58 in the presence of 2 M TMAO could be due to sequence specific stabilization by TMAO.

Sequence segment 71−81 (β strand 5) exchanges out in two kinetic phases. Quantitative analysis shows that during the fast and slow phases of noncooperative exchange it exchanges out in the EX2 regime and EXX regime of HX, respectively (Figure 5 and Table S2). This could possibly be due to the nature of hydrogen bonding of β strand 5. β strand 5 has two groups of amide sites, one that is hydrogen bonded to β strand 1 and another that is solvent exposed and not involved in hydrogen bonding. This could lead to an order of magnitude difference in the observed apparent rate constants for the two kinetic phases of HX.

Native State Dynamics in the Presence of TMAO and Urea. In natural environments, many organisms may face challenging conditions such as a high concentration of urea, a high temperature, or a high salt concentration.[14] Furthermore, the cellular milieu is crowded because of the presence of a variety of macromolecules.[15] To deal with protein denaturing environmental conditions and to maintain functionally relevant macromolecular states, organisms synthesize many small molecules. An osmolyte such as urea destabilizes proteins by being preferentially enriched at the protein surface, presumably because it binds to the polypeptide backbone,[20,67−70] while TMAO stabilizes proteins by being preferentially excluded from the polypeptide backbone.[17,71] Hence, urea and TMAO are a special pair of cosolvent osmolytes that are found in nature and that counteract each other in their effects on the dynamics of the polypeptide backbone.

The PI3K SH3 domain has been found to sample the same conformational space in the absence and presence of urea.[13] In the presence of increasing concentrations of urea, the cooperativity of unfolding increases. Until now, it was not known whether TMAO affects the cooperativity of protein unfolding. This study shows that by reducing the cooperativity of unfolding, TMAO counters the effect of urea not only on stability but also on cooperativity. Furthermore, it also shows that in the presence of TMAO local fluctuations dominate over global unfolding events. The ability of TMAO to counteract the effect of urea on polypeptide backbone dynamics may be important in restoring the functionally relevant backbone fluctuations that are important for protein function.[72]

Testing the Model for Thermodynamic Stability and Cooperativity. Proteins are marginally stable molecules. Because of this marginal stability, the native state of a protein samples many partially unfolded to completely unfolded conformations. It is not understood whether a protein switches from one conformation to another by cooperative structural opening or by a gradual noncooperative structural opening. However, a recent study has shown that the cooperativity of structural opening can be modulated by changing the stabilities of the unfolded state by adding a denaturant.[13] Subsequent studies have shown that protein destabilizing conditions such as a high pH[11] or a mutation[12] also increase the cooperativity of unfolding.

These observations suggest that an increase in cooperativity of unfolding is due to the decrease in the stability of the protein. To confirm the connection established between protein stability and cooperativity, it had become important to establish that stabilization of the protein would lead to a decrease in the cooperativity of unfolding. This study shows that this is indeed the case: stabilization of the PI3K SH3 domain upon addition of the osmolyte TMAO is accompanied by switching of the inherently cooperative unfolding reaction of the PI3K SH3 domain to a completely noncooperative unfolding reaction.

■ CONCLUSION

This study provides important new insight into the dynamic relationship between thermodynamic stability and the cooperativity of protein folding. The extent of cooperativity of the unfolding of the PI3K SH3 domain decreases upon addition of the stabilizing osmolyte TMAO: fewer amide sites exchange out cooperatively as the concentration of TMAO present during HX is increased. In the presence of 2 M TMAO, cooperativity is completely lost as the protein is very strongly stabilized: all amide sites undergo HX in a noncorrelated (noncooperative) manner. The protein then

DOI: 10.1021/acs.biochem.8b00698
Biochemistry 2018, 57, 5851−5863

unfolds in a completely noncooperative, uphill manner, suggesting that refolding under such strongly stabilizing native conditions would also be completely noncooperative, but downhill. It is important to note that the concentrations of TMAO at which its effect on cooperativity is seen are similar to concentrations of TMAO found in the cells of marine organisms.[14]

■ ASSOCIATED CONTENT

Supporting Information

The Supporting Information is available free of charge on the ACS Publications website at DOI: 10.1021/acs.biochem.8b00698.

Mechanism of HX, equations for analyzing the equilibrium unfolding curves as well as the kinetics of HX, mass spectrometric and spectroscopic characterization of the protein in the presence of TMAO, kinetics of HX and peak width analysis for the intact protein as well as for different sequence segments, and tables summarizing HX into the intact protein and the different sequence segments (PDF)

■ AUTHOR INFORMATION

Corresponding Author

*Indian Institute of Science Education and Research, Pune 411008, India. E-mail: jayant@iiserpune.ac.in. Telephone: 91-20-25908008.

ORCID

Prashant N. Jethva: 0000-0002-7704-2810

Jayant B. Udgaonkar: 0000-0002-7005-224X

Author Contributions

P.N.J. designed and carried out the experiments. P.N.J. and J.B.U. analyzed the results. P.N.J. and J.B.U. wrote the manuscript. The final version of the manuscript was approved by both authors.

Funding

J.B.U. is a recipient of a J. C. Bose National Fellowship from the Government of India. This work was funded by the Tata Institute of Fundamental Research and by the Department of Biotechnology, Government of India.

Notes

The authors declare no competing financial interest.

■ ACKNOWLEDGMENTS

The authors thank members of our laboratory for discussion and for their comments on the manuscript and Pooja Malhotra for critical reading of the manuscript.

■ REFERENCES

(1) Linderstrøm Lang, K. U., and Schellman, J. A. (1959) Protein Structure and Enzyme Activity. In *The Enzymes*, 2nd ed., Vol. *1*, Academic Press, New York.

(2) McCammon, J. A., Gelin, B. R., and Karplus, M. (1977) Dynamics of folded proteins. *Nature 267*, 585−590.

(3) Frauenfelder, H., Parak, F., and Young, R. D. (1988) Conformational substates in proteins. *Annu. Rev. Biophys. Biophys. Chem. 17*, 451−479.

(4) Epstein, D. M., Benkovic, S. J., and Wright, P. E. (1995) Dynamics of the dihydrofolate reductase-folate complex: catalytic sites and regions known to undergo conformational change exhibit diverse dynamical features. *Biochemistry 34*, 11037−11048.

(5) Henzler-Wildman, K., and Kern, D. (2007) Dynamic personalities of proteins. *Nature 450*, 964−972.

(6) Malhotra, P., and Udgaonkar, J. B. (2014) High energy intermediates in protein unfolding characterized by thiol labeling under nativelike conditions. *Biochemistry 53*, 3608−3620.

(7) Chan, H. S., Zhang, Z., Wallin, S., and Liu, Z. (2011) Cooperativity, local-nonlocal coupling, and nonnative interactions: principles of protein folding from coarse-grained models. *Annu. Rev. Phys. Chem. 62*, 301−326.

(8) Dill, K. A., Fiebig, K. M., and Chan, H. S. (1993) Cooperativity in protein-folding kinetics. *Proc. Natl. Acad. Sci. U. S. A. 90*, 1942−1946.

(9) Chan, H. S., Bromberg, S., and Dill, K. A. (1995) Models of cooperativity in protein folding. *Philos. Trans. R. Soc., B 348*, 61−70.

(10) Canchi, D. R., and García, A. E. (2013) Cosolvent effects on protein stability. *Annu. Rev. Phys. Chem. 64*, 273−293.

(11) Malhotra, P., and Udgaonkar, J. B. (2015) Tuning cooperativity on the free energy landscape of protein folding. *Biochemistry 54*, 3431−3441.

(12) Malhotra, P., Jethva, P. N., and Udgaonkar, J. B. (2017) Chemical denaturants smoothen ruggedness on the free energy landscape of protein folding. *Biochemistry 56*, 4053−4063.

(13) Jethva, P. N., and Udgaonkar, J. B. (2017) Modulation of the extent of cooperative structural change during protein folding by chemical denaturant. *J. Phys. Chem. B 121*, 8263−8275.

(14) Yancey, P. H., Clark, M. E., Hand, S. C., Bowlus, R. D., and Somero, G. N. (1982) Living with water stress: evolution of osmolyte systems. *Science 217*, 1214−1222.

(15) Somero, G. (1986) Protons, osmolytes, and fitness of internal milieu for protein function. *Am. J. Physiol. Regul. Integr. Comp. Physiol. 251*, R197−R213.

(16) Yancey, P. H., and Somero, G. N. (1979) Counteraction of urea destabilization of protein structure by methylamine osmoregulatory compounds of elasmobranch fishes. *Biochem. J. 183*, 317−323.

(17) Liu, Y., and Bolen, D. (1995) The peptide backbone plays a dominant role in protein stabilization by naturally occurring osmolytes. *Biochemistry 34*, 12884−12891.

(18) Baskakov, I., and Bolen, D. W. (1998) Forcing thermodynamically unfolded proteins to fold. *J. Biol. Chem. 273*, 4831−4834.

(19) Zou, Q., Bennion, B. J., Daggett, V., and Murphy, K. P. (2002) The molecular mechanism of stabilization of proteins by TMAO and its ability to counteract the effects of urea. *J. Am. Chem. Soc. 124*, 1192−1202.

(20) Auton, M., and Bolen, D. W. (2005) Predicting the energetics of osmolyte-induced protein folding/unfolding. *Proc. Natl. Acad. Sci. U. S. A. 102*, 15065−15068.

(21) Cho, S. S., Reddy, G., Straub, J. E., and Thirumalai, D. (2011) Entropic stabilization of proteins by TMAO. *J. Phys. Chem. B 115*, 13401−13407.

(22) Ma, J., Pazos, I. M., and Gai, F. (2014) Microscopic insights into the protein-stabilizing effect of trimethylamine N-oxide (TMAO). *Proc. Natl. Acad. Sci. U. S. A. 111*, 8476−8481.

(23) Pradeep, L., and Udgaonkar, J. B. (2004) Osmolytes induce structure in an early intermediate on the folding pathway of barstar. *J. Biol. Chem. 279*, 40303−40313.

(24) Qu, Y., Bolen, C., and Bolen, D. (1998) Osmolyte-driven contraction of a random coil protein. *Proc. Natl. Acad. Sci. U. S. A. 95*, 9268−9273.

(25) Uversky, V. N., Li, J., and Fink, A. L. (2001) Trimethylamine-N-oxide-induced folding of α-synuclein. *FEBS Lett. 509*, 31−35.

(26) Ferreon, A. C. M., Moosa, M. M., Gambin, Y., and Deniz, A. A. (2012) Counteracting chemical chaperone effects on the single-molecule α-synuclein structural landscape. *Proc. Natl. Acad. Sci. U. S. A. 109*, 17826−17831.

(27) Malhotra, P., and Udgaonkar, J. B. (2016) How cooperative are protein folding and unfolding transitions? *Protein Sci. 25*, 1924−1941.

(28) Bai, Y., Sosnick, T. R., Mayne, L., and Englander, S. W. (1995) Protein folding intermediates: native-state hydrogen exchange. *Science 269*, 192−197.

DOI: 10.1021/acs.biochem.8b00698
Biochemistry 2018, 57, 5851−5863

(29) Chamberlain, A. K., Handel, T. M., and Marqusee, S. (1996) Detection of rare partially folded molecules in equilibrium with the native conformation of RNaseH. *Nat. Struct. Mol. Biol. 3*, 782−787.
(30) Sridevi, K., and Udgaonkar, J. B. (2002) Unfolding rates of barstar determined in native and low denaturant conditions indicate the presence of intermediates. *Biochemistry 41*, 1568−1578.
(31) Jha, S. K., Dasgupta, A., Malhotra, P., and Udgaonkar, J. B. (2011) Identification of multiple folding pathways of monellin using pulsed thiol labeling and mass spectrometry. *Biochemistry 50*, 3062−3074.
(32) Korzhnev, D. M., Salvatella, X., Vendruscolo, M., Di Nardo, A. A., Davidson, A. R., Dobson, C. M., and Kay, L. E. (2004) Low-populated folding intermediates of Fyn SH3 characterized by relaxation dispersion NMR. *Nature 430*, 586−590.
(33) Neudecker, P., Robustelli, P., Cavalli, A., Walsh, P., Lundström, P., Zarrine-Afsar, A., Sharpe, S., Vendruscolo, M., and Kay, L. E. (2012) Structure of an intermediate state in protein folding and aggregation. *Science 336*, 362−366.
(34) Miranker, A., Robinson, C. V., Radford, S. E., Aplin, R. T., and Dobson, C. M. (1993) Detection of transient protein folding populations by mass spectrometry. *Science 262*, 896−900.
(35) Yi, Q., and Baker, D. (1996) Direct evidence for a two-state protein unfolding transition from hydrogen-deuterium exchange, mass spectrometry, and NMR. *Protein Sci. 5*, 1060−1066.
(36) Ferraro, D. M., Lazo, N. D., and Robertson, A. D. (2004) EX1 hydrogen exchange and protein folding. *Biochemistry 43*, 587−594.
(37) Jackson, S. E. (1998) How do small single-domain proteins fold? *Folding Des. 3*, R81−R91.
(38) Koch, C. A., Anderson, D., Moran, M. F., Ellis, C., and Pawson, T. (1991) SH2 and SH3 domains: elements that control interactions of cytoplasmic signaling proteins. *Science 252*, 668−674.
(39) Kuriyan, J., and Cowburn, D. (1997) Modular peptide recognition domains in eukaryotic signaling. *Annu. Rev. Biophys. Biomol. Struct. 26*, 259−288.
(40) Guijarro, J. I., Morton, C. J., Plaxco, K. W., Campbell, I. D., and Dobson, C. M. (1998) Folding kinetics of the SH3 domain of PI3 kinase by real-time NMR combined with optical spectroscopy. *J. Mol. Biol. 276*, 657−667.
(41) Wani, A. H., and Udgaonkar, J. B. (2009) Revealing a concealed intermediate that forms after the rate-limiting step of refolding of the SH3 domain of PI3 kinase. *J. Mol. Biol. 387*, 348−362.
(42) Dasgupta, A., and Udgaonkar, J. B. (2012) Four-state folding of a SH3 domain: Salt-induced modulation of the stabilities of the intermediates and native state. *Biochemistry 51*, 4723−4734.
(43) Dasgupta, A., and Udgaonkar, J. B. (2012) Transient non-native burial of a Trp residue occurs initially during the unfolding of a SH3 domain. *Biochemistry 51*, 8226−8234.
(44) Kishore, M., Krishnamoorthy, G., and Udgaonkar, J. B. (2013) Critical evaluation of the two-state model describing the equilibrium unfolding of the PI3K SH3 domain by time-resolved fluorescence resonance energy transfer. *Biochemistry 52*, 9482−9496.
(45) Aghera, N., and Udgaonkar, J. B. (2017) Stepwise assembly of β-sheet structure during the folding of an SH3 domain revealed by a pulsed hydrogen exchange mass spectrometry study. *Biochemistry 56*, 3754−3769.
(46) Sen, S., Goluguri, R. R., and Udgaonkar, J. B. (2017) A dry transition state more compact than the native state is stabilized by non-native interactions during the unfolding of a small protein. *Biochemistry 56*, 3699−3703.
(47) Wani, A. H., and Udgaonkar, J. B. (2009) Native state dynamics drive the unfolding of the SH3 domain of PI3 kinase at high denaturant concentration. *Proc. Natl. Acad. Sci. U. S. A. 106*, 20711−20716.
(48) Wang, A., and Bolen, D. (1997) A naturally occurring protective system in urea-rich cells: mechanism of osmolyte protection of proteins against urea denaturation. *Biochemistry 36*, 9101−9108.
(49) Bader, R., Bamford, R., Zurdo, J., Luisi, B. F., and Dobson, C. M. (2006) Probing the mechanism of amyloidogenesis through a tandem repeat of the PI3-SH3 domain suggests a generic model for protein aggregation and fibril formation. *J. Mol. Biol. 356*, 189−208.
(50) Guttman, M., Weis, D. D., Engen, J. R., and Lee, K. K. (2013) Analysis of overlapped and noisy hydrogen/deuterium exchange mass spectra. *J. Am. Soc. Mass Spectrom. 24*, 1906−1912.
(51) Weis, D. D., Engen, J. R., and Kass, I. J. (2006) Semi-automated data processing of hydrogen exchange mass spectra using HX-Express. *J. Am. Soc. Mass Spectrom. 17*, 1700−1703.
(52) Weis, D. D., Wales, T. E., Engen, J. R., Hotchko, M., and Ten Eyck, L. F. (2006) Identification and characterization of EX1 kinetics in H/D exchange mass spectrometry by peak width analysis. *J. Am. Soc. Mass Spectrom. 17*, 1498−1509.
(53) Wales, T. E., and Engen, J. R. (2006) Partial unfolding of diverse SH3 domains on a wide timescale. *J. Mol. Biol. 357*, 1592−1604.
(54) Engen, J. R., Wales, T. E., Chen, S., Marzluff, E. M., Hassell, K. M., Weis, D. D., and Smithgall, T. E. (2013) Partial cooperative unfolding in proteins as observed by hydrogen exchange mass spectrometry. *Int. Rev. Phys. Chem. 32*, 96−127.
(55) Arrington, C. B., Teesch, L. M., and Robertson, A. D. (1999) Defining protein ensembles with native-state NH exchange: kinetics of interconversion and cooperative units from combined NMR and MS analysis. *J. Mol. Biol. 285*, 1265−1275.
(56) Xiao, H., Hoerner, J. K., Eyles, S. J., Dobo, A., Voigtman, E., Mel'čuk, A. I., and Kaltashov, I. A. (2005) Mapping protein energy landscapes with amide hydrogen exchange and mass spectrometry: I. A generalized model for a two-state protein and comparison with experiment. *Protein Sci. 14*, 543−557.
(57) Krishna, M. M., Hoang, L., Lin, Y., and Englander, S. W. (2004) Hydrogen exchange methods to study protein folding. *Methods 34*, 51−64.
(58) Wei, G., Xi, W., Nussinov, R., and Ma, B. (2016) Protein ensembles: how does nature harness thermodynamic fluctuations for life? The diverse functional roles of conformational ensembles in the cell. *Chem. Rev. 116*, 6516−6551.
(59) Eisenmesser, E. Z., Millet, O., Labeikovsky, W., Korzhnev, D. M., Wolf-Watz, M., Bosco, D. A., Skalicky, J. J., Kay, L. E., and Kern, D. (2005) Intrinsic dynamics of an enzyme underlies catalysis. *Nature 438*, 117−121.
(60) Engen, J. R., Smithgall, T. E., Gmeiner, W. H., and Smith, D. L. (1997) Identification and localization of slow, natural, cooperative unfolding in the hematopoietic cell kinase SH3 domain by amide hydrogen exchange and mass spectrometry. *Biochemistry 36*, 14384−14391.
(61) Udgaonkar, J. B. (2008) Multiple routes and structural heterogeneity in protein folding. *Annu. Rev. Biophys. 37*, 489−510.
(62) Roder, H., and Colón, W. (1997) Kinetic role of early intermediates in protein folding. *Curr. Opin. Struct. Biol. 7*, 15−28.
(63) Canet, D., Last, A. M., Tito, P., Sunde, M., Spencer, A., Archer, D. B., Redfield, C., Robinson, C. V., and Dobson, C. M. (2002) Local cooperativity in the unfolding of an amyloidogenic variant of human lysozyme. *Nat. Struct. Biol. 9*, 308−315.
(64) Gruebele, M. (2005) Downhill protein folding: evolution meets physics. *C. R. Biol. 328*, 701−712.
(65) Lin, S. L., Zarrine-Afsar, A., and Davidson, A. R. (2009) The osmolyte trimethylamine-N-oxide stabilizes the Fyn SH3 domain without altering the structure of its folding transition state. *Protein Sci. 18*, 526−536.
(66) Booker, G. W., Gout, I., Downing, K. A., Driscoll, P. C., Boyd, J., Waterfield, M. D., and Campbell, I. D. (1993) Solution structure and ligand-binding site of the SH3 domain of the p85α subunit of phosphatidylinositol 3-kinase. *Cell 73*, 813−822.
(67) Tirado-Rives, J., Orozco, M., and Jorgensen, W. L. (1997) Molecular dynamics simulations of the unfolding of barnase in water and 8 M aqueous urea. *Biochemistry 36*, 7313−7329.
(68) Auton, M., Holthauzen, L. M. F., and Bolen, D. W. (2007) Anatomy of energetic changes accompanying urea-induced protein denaturation. *Proc. Natl. Acad. Sci. U. S. A. 104*, 15317−15322.

DOI: 10.1021/acs.biochem.8b00698
Biochemistry 2018, 57, 5851−5863

(69) Hua, L., Zhou, R., Thirumalai, D., and Berne, B. (2008) Urea denaturation by stronger dispersion interactions with proteins than water implies a 2-stage unfolding. *Proc. Natl. Acad. Sci. U. S. A. 105*, 16928−16933.
(70) Lim, W. K., Rösgen, J., and Englander, S. W. (2009) Urea, but not guanidinium, destabilizes proteins by forming hydrogen bonds to the peptide group. *Proc. Natl. Acad. Sci. U. S. A. 106*, 2595−2600.
(71) Bolen, D. (2004) Effects of naturally occurring osmolytes on protein stability and solubility: issues important in protein crystallization. *Methods 34*, 312−322.
(72) Doan-Nguyen, V., and Loria, J. P. (2007) The effects of cosolutes on protein dynamics: The reversal of denaturant-induced protein fluctuations by trimethylamine N-oxide. *Protein Sci. 16*, 20−29.

DOI: 10.1021/acs.biochem.8b00698
Biochemistry 2018, 57, 5851−5863